Prdm5 suppresses Apc^{Min}-driven intestinal adenomas and regulates monoacylglycerol lipase expression.

Prdm5 suppresses Apc^{Min}-driven intestinal adenomas and regulates monoacylglycerol lipase expression

G G Galli[1,7,8], H A Multhaupt[2], M Carrara[3], K H de Lichtenberg[1], I B J Christensen[4], D Linnemann[5], E Santoni-Rugiu[6], R A Calogero[3] and A H Lund[1]

[1]Biotech Research and Innovation Centre, Centre for Epigenetics, University of Copenhagen, Copenhagen, Denmark
[2]Department of Biomedical Sciences, University of Copenhagen, Copenhagen, Denmark
[3]Department of Clinical and Biological Sciences, Molecular Biotechnology Center, University of Torino, Torino, Italy
[4]The Finsen Laboratory, Faculty of Health Sciences, Rigshospitalet, University of Copenhagen, Copenhagen, Denmark
[5]Department of Pathology, Herlev Hospital, Herlev, Denmark
[6]Department of Pathology, Diagnostic Center, Righospitalet, Copenhagen, Denmark
Correspondence: Professor AH Lund, Biotech Research and Innovation Centre (BRIC), Centre for Epigenetics, University of Copenhagen, Ole Maaloes Vej 5, Copenhagen DK-2200, Denmark. E-mail: anders.lund@bric.ku.dk

Abstract

PRDM proteins are tissue-specific transcription factors often deregulated in diseases, particularly in cancer where different members have been found to act as oncogenes or tumor suppressors. PRDM5 is a poorly characterized member of the PRDM family for which several studies have reported a high frequency of promoter hypermethylation in cancer types of gastrointestinal origin. We report here the characterization of Prdm5 knockout mice in the context of intestinal carcinogenesis. We demonstrate that loss of *Prdm5* increases the number of adenomas throughout the murine small intestine on an Apc^{Min} background. By using the genome-wide ChIP-seq (chromatin immunoprecipitation (ChIP) followed by DNA sequencing) and transcriptome analyses we identify loci encoding proteins involved in metabolic processes as prominent PRDM5 targets and characterize monoacylglycerol lipase (*Mgll*) as a direct PRDM5 target in human colon cancer cells and in *Prdm5* mutant mouse intestines. Moreover, we report the downregulation of PRDM5 protein expression in human colon neoplastic lesions. In summary, our data provide the first causal link between *Prdm5* loss and intestinal carcinogenesis, and uncover an extensive and novel PRDM5 target repertoire likely facilitating the tumor-suppressive functions of PRDM5.

Introduction

PRDM5 is a poorly characterized member of the PRDM family of transcriptional regulators. The members of this family are known to influence tissue-specific differentiation, and many members have been found mutated or deregulated in pathological conditions. This has been demonstrated most prominently in cancer, where different PRDM proteins have been shown to act either as oncogenes or tumor suppressors.[1]

Several reports have suggested that *PRDM5* is mutated or silenced in human diseases. Rare mutations have been found in *PRDM5* in neutropenia[2] and brittle cornea syndrome,[3] whereas some studies propose tumor-suppressive functions for PRDM5 due to its silencing in a variety of cancer cell lines and clinical samples.[4, 5, 6, 7, 8] Silencing mechanisms include DNA methylation of a CpG island associated with the *PRDM5* locus and the increased abundance of the H3K27me3-repressive epigenetic mark at the promoter region.[8] Interestingly, PRDM5 silencing has been shown to occur with high frequency in samples from patients with gastric dysplasia or early gastric cancer.[7]

Regarding its molecular mechanism, PRDM5 is a sequence-specific transcriptional regulator[2, 9] encompassing an N-terminal PR domain, for which no histone methyltransferase activity has been detected, and 16 C_2H_2 zinc-finger domains mediating protein–DNA and protein–protein interactions.[2] A multitude of genes have been reported to be regulated by PRDM5 including a large repertoire of genes

involved in carcinogenesis such as *p53*, *MYC* and *MDM2*,[2, 6] although an extensive characterization of PRDM5 targets in relevant cancer settings is still lacking.

Recent studies have suggested Prdm5 to be a negative regulator of the WNT pathway.[6, 10] Indeed, Prdm5 knockdown in zebrafish was shown to be embryonically lethal and to enhance the masterblind phenotype resulting from an Axin heterozygous mutation.[10] In cancer samples, the methylation status of *PRDM5* was shown to negatively correlate with the β-catenin expression level,[6] and PRDM5 expression represses a WNT-specific transcriptional reporter.[6] Aberrant activation of the WNT signaling is implicated in driving the formation of various human cancer types, predominantly of the gastrointestinal origin.[11] In particular, colorectal cancers can arise from hereditary predisposition syndromes such as familial adenomatous polyposis, a condition that involves the formation of benign polyps throughout the small intestine. The disease is driven by mutations in the *APC* tumor-suppressor gene,[12] which are found in ~80% of the colon cancer cases.[13] APC is a large protein component of the 'destruction complex', which mediates proteasome-dependent β-catenin degradation[14] and APC mutations in humans, as well as in mouse models, resulting in aberrant activation of the WNT signaling[15] and polyposis.[16] The transition from adenomas to advanced cancer types requires additional genetic events involving known oncogenes or tumor suppressors such as *KRAS* or *p53*.[13]

To investigate functional links between Prdm5 silencing and cancer development, we analyzed a *Prdm5* loss-of-function mouse model from a pathological perspective and, although Prdm5 does not seem to be implicated in p53-driven lymphomagenesis, we found the loss of Prdm5 to accelerate Apc^{Min}-driven intestinal polyposis. Using high-throughput RNA sequencing and genome-wide mapping of Prdm5-binding sites in colon cancer cells, we identified a set of metabolic genes as targeted by Prdm5. In mouse cells and the intestine, monoacylglycerol lipase (*Mgll*) is a Prdm5 functional target that is synergistically upregulated upon *Prdm5* loss and WNT pathway activation. Moreover, we demonstrate that the PRDM5 protein is downregulated in early stages of human colon carcinogenesis, further tying PRDM5 loss to intestinal polyposis.

Results

Prdm5 loss increases intestinal adenomas driven by Apc mutation

PRDM5 mutations and deregulations have been associated with different diseases such as neutropenia,[2] brittle cornea syndrome[3] and various types of cancers.[4, 5, 6, 7, 8] As no causality has been described so far, we undertook the analysis of a *Prdm5* gene trap mouse model (named $Prdm5^{LacZ/LacZ}$[9]) in different pathological settings, particularly cancer.

As previously reported, Prdm5 mutant mice display a bone developmental defect but are otherwise morphologically normal.[9] We analyzed cohorts of $Prdm5^{LacZ/LacZ}$ animals at different ages but did not observe neoplasias by gross pathology up to the age of 70 weeks. We thereby hypothesized that Prdm5 enhances tumorigenesis driven by the activation of known cancer pathways. As MDM2 was shown to be regulated by PRDM5[6] and *p53* is among its published target genes,[2] we evaluated whether Prdm5 loss might accelerate tumorigenesis induced by p53 loss. p53 knockout animals developed predominantly B-cell lymphomas, with a mean latency of ~5 months, whereas heterozygous mice developed a broader spectrum of cancer types including sarcomas with an average latency of 1 year, as previously reported.[17] As depicted in Figure 1a, *Prdm5* loss did not accelerate the occurrence of lymphomas or changed the range of neoplasms significantly in either a p53 knockout or p53 heterozygous background (Figure 1a and data not shown).

Figure 1.

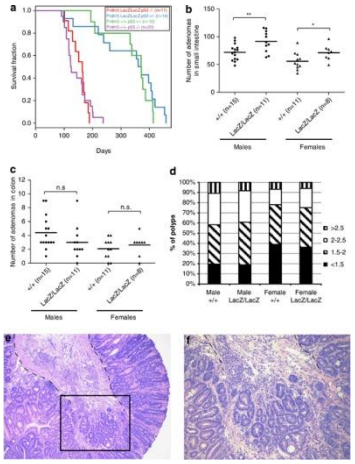

Prdm5 loss increases the number of adenomas and microinvasion foci in the *Apc*^{Min} mouse model. (**a**) Kaplan–Meier survival curve from mice cohorts resulting from *Prdm5*$^{+/LacZ}$*p53*$^{+/-}$ crosses. (**b**–**c**) Number of adenomas observed in the small intestine (**b**) and colon (**c**) of mouse cohorts from *Prdm5*$^{+/LacZ}$*;Apc*^{Min} crosses. (**P<0.01, *P<0.05). (**d**) Size of observed adenomas classified according to diameter ranges in millimeters. (**e**) HE-staining of an example of a large adenoma from a *Prdm5*$^{LacZ/LacZ}$*;Apc*^{Min} animal displaying microinvasion foci (× 10) and (**f**) higher magnification (× 20). Black dashed lines indicate regions where epithelium/submucosa structure is preserved.

Given the reported promoter hypermethylation of *PRDM5* in gastrointestinal cancer types, we proceeded to analyze possible tumor-suppressive functions for Prdm5 in the intestine. Activation of the WNT pathway is a prominent factor in the early stages of intestinal carcinogenesis,[11] and PRDM5 was shown to be a negative regulator of the WNT signaling in both zebrafish[10] and human cell culture systems.[6]

To evaluate the impact of Prdm5 loss on intestinal neoplasia induced by constitutive WNT pathway activation, we crossed *Prdm5*$^{LacZ/LacZ}$ mice with the *Apc*^{min} tumor-prone strain.[18] The *Apc*^{Min} mouse model was generated by random mutagenesis screening and bears a point mutation at the codon 850 of the *Apc* gene, phenotypically resulting in the formation of a multiple intestinal polyps (min) particularly in the small intestine.[18] The *Prdm5*^{LacZ} allele segregates in normal Mendelian ratios in the *Apc*^{Min} background (data not shown), excluding the possibility of major developmental defects induced by Prdm5 loss in an *Apc* mutant background. To analyze an effect of Prdm5 loss on polyp formation, we killed cohorts of male and female *Apc*^{min} mice wild type or mutant for Prdm5 at 20 weeks of age and quantified adenomas in the intestines. Interestingly, we observed a significant increase in the number of polyps in *Prdm5*$^{LacZ/LacZ}$*; Apc*^{Min} mice compared with *Prdm5*$^{+/+}$*; Apc*^{Min} controls for both sexes (Figure 1b). This effect was specific for the small intestine compared with the colon (Figure 1c). Histological examination revealed that all mice developed tubular adenomas with moderate to severe dysplasia. Although no differences in the distribution of the size of the adenomas were observed (Figure 1d), an increased number of *Prdm5*$^{LacZ/LacZ}$*; Apc*^{Min} animals displayed microinvasion foci associated with intestinal adenomas compared with *Prdm5*$^{+/+}$*;Apc*^{Min} animals (7/19 *Prdm5*$^{LacZ/LaczZ}$*; Apc*^{Min} and 2/27 *Prdm5*$^{+/+}$*; Apc*^{Min}, P<0.022 Fisher's exact test) (Figures 1e and f). These results demonstrate that *Prdm5* loss has an impact on the multiplicity of adenomas upon aberrant WNT signaling and, to lesser extent, on the aggressiveness of the developed dysplasia, providing the first genetic evidence for a tumor-suppressive function of *Prdm5*.

Prdm5 regulates metabolic genes in intestinal cancer cells

To unveil the molecular functions of Prdm5 in intestinal cells and to understand how it attenuates *Apc*^{Min}-driven intestinal polyposis, we analyzed genes that are regulated following *PRDM5* silencing in cultured

cells. We employed Caco-2 cells, as this is one of the few intestinal cancer cell lines tested, which retain detectable PRDM5 levels (data not shown). The small interfering RNA-mediated knockdown of *PRDM5* efficiently reduced *PRDM5* mRNA and protein levels (Figure 2a), and we isolated RNA 72 h after treatment to analyze the transcriptome by RNA sequencing. Bioinformatic analyses retrieved 5170 differentially expressed genes (*q*-value <0.05, represented in gray in Figure 2b), out of which 177 displayed regulation higher than two-fold changes (in black in Figure 2b), indicating that PRDM5 loss does not elicit a strong transcriptional response. Surprisingly, functional annotation of genes deregulated with a fold change >1.5 showed an enrichment for genes involved in metabolic pathways such as lipid and acylglycerol (Figure 2c). We could indeed verify that a set of genes involved in various metabolic processes were deregulated upon *PRDM5* silencing in independent sets of experiments (Figure 2d). In summary, our results demonstrate that *PRDM5* loss might impair the expression of metabolic pathways in cancer cells.

Figure 2.

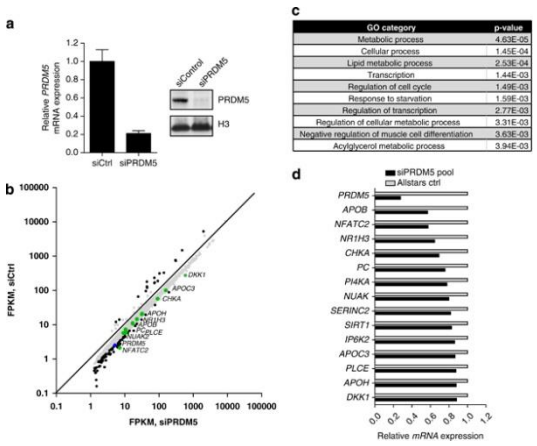

PRDM5 silencing modulates the expression of metabolic genes in Caco-2 cells. (**a**) qPCR (left panel) and western blot (right panel) analysis displaying PRDM5 expression levels in Caco-2 cells treated with control (siCtrl) or PRDM5 small interfering RNAs (siPRDM5). H3 was used as the loading control. (**b**) Expression levels in FPKM (fragments per kilobase of exon per million fragments mapped) of genes deregulated upon *PRDM5* knockdown with *q*-value <0.05 (gray dots). Genes deregulated more than two-fold are displayed as black dots; *PRDM5* and genes involved in metabolic processes are highlighted in blue and green, respectively. (**c**) Gene ontology analysis of deregulated genes with *q*-value <0.05 and fold change >1.5. (**d**) Technical validation by qPCR for the expression of metabolic genes in an independent set of Caco-2 cells transfected with control (gray bars) or siPRDM5 oligos (black bars).

PRDM5 binds the transcription start site of metabolic genes in intestinal cells

To understand whether PRDM5 could directly target metabolic genes to regulate their expression, we performed chromatin immunoprecipitation for PRDM5 in Caco-2 cells followed by sequencing (ChIP-seq).

We performed ChIPs using two independent PRDM5 polyclonal antibodies. After mapping of sequencing reads (~30 millions of uniquely mapped reads were obtained for each reaction), we performed peak finding using an immunoglobulin G (IgG) sample as negative control and overlaid the results retrieved from the two PRDM5 antibodies. We obtained 1413 high-confidence PRDM5-binding sites (Figure 3a and Supplementary Table S1), of which approximately half were located within 1 kb of the closest annotated transcription start site (Figure 3b). Indeed, the signal distribution of PRDM5 was mainly localized around the transcriptional start site (TSS) of its target genes and, to a lesser extent, in gene bodies (Figure 3c). Gene ontology analysis of the top 500 hits from our ChIP-seq revealed that PRDM5 targeted genes involved in metabolic processes and gene expression regulation (Figure 3d). Indeed, by using ChIP-qPCR on an independent chromatin preparation, we validated PRDM5 binding to the TSS of a number of metabolic enzymes compared with IgG

and negative regions selected from ChIP-seq (Figure 3e). These data suggest that, at least in this cellular system, PRDM5 actively targets proximal promoters of genes involved in metabolic pathways.

Figure 3.

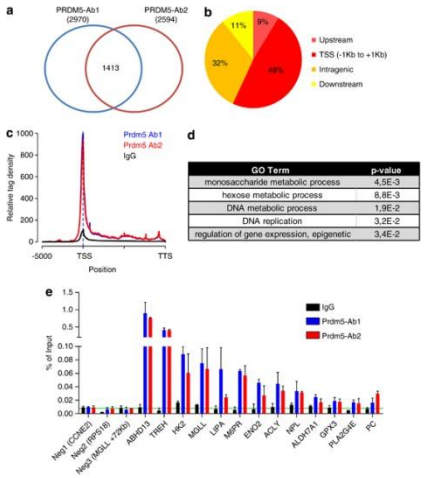

PRDM5 targets loci encoding metabolic enzymes in colon cancer cells. (**a**) Venn diagram representing the number of ChIP-seq peaks obtained from peak finding with each PRDM5 antibody and their overlap. (**b**) Distribution of the position of PRDM5 peaks with respect to TSSs. (**c**) The mean distribution of tags across gene bodies for PRDM5 ChIP-seq (PRDM5-ab1 in blue, PRDM5-ab2 in red and IgG (immunoglobulin G) in black). Vertical dashed line at x=0 represents the TSS. Positions after the TSS are represented as % of the length of the gene. (**d**) Gene ontology enrichment for Biological processes of the top PRDM5 targets (reads number cutoff >100). (**e**) ChIP-qPCR validation of PRDM5 peaks in selected genes or negative control regions from an independent chromatin preparation immunoprecipitated with IgG, PRDM5-Ab1 or PRDM5-Ab2 (in black, blue and red, respectively). Green horizontal line represents the average 'noise' value obtained by ChIP-qPCR on a set of negative regions.

Mgll is a WNT-responsive gene and a functional Prdm5 target

In order to identify which PRDM5 target gene could be critical in its suppression of Apc^{Min}-driven polyposis in mouse cells, we performed a microarray analysis of wild-type and $Prdm5^{LacZ/LacZ}$ mouse embryonic fibroblasts (MEFs). We selected such a model system, as *Prdm5* mutant fibroblasts display an increased expression of total β-catenin protein, further confirming the role of Prdm5 as a negative regulator of the WNT signaling (Figure 4a). Statistical analysis revealed 472 differentially expressed probe sets, with a fold change cutoff of 1.5 and a *P*-value <0.05 (Supplementary Table S3). We applied a stringent validation strategy and focused on genes involved in carcinogenesis. Among the responsive genes we identified *Adamts9*, *Col1a1*, *Mmp13* and *Mgll* as genes robustly regulated by Prdm5 in MEFs (Figure 4b). Importantly, tumor-suppressor genes such as *Adamts9* and *Col1a1* were repressed (we recently reported the latter as a functional Prdm5 target in osteoblasts[9]), whereas genes involved in cancer progression and invasion such as *Mmp13* and *Mgll* were upregulated. We did not detect the differential expression for *Dkk1* (Figure 4b), suggesting species- and/or cell-specific regulation of this previously identified target.[10]

Figure 4.

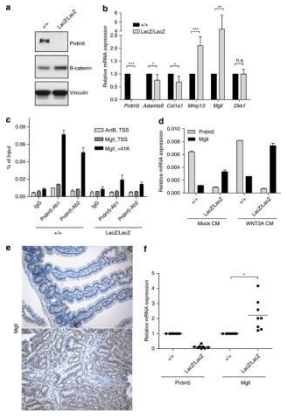

Mgll is a WNT-responsive gene regulated by Prdm5 *in vivo*. (**a**) Western blot analysis of wild-type and *Prdm5*$^{LacZ/LacZ}$ MEFs with indicated antibodies. Vinculin is used for equal protein loading. (**b**) qPCR validation of the microarray analysis of a set of deregulated genes from Prdm5 mutant MEFs (n=6 per group). ***P<0.005, **P<0.01, *P<0.05 according to unpaired t-test. (**c**) ChIP-qPCR in wild-type and *Prdm5*$^{LacZ/LacZ}$ MEFs with indicated antibodies. ActB_TSS is used as the negative control region. (**d**) *Prdm5* and *Mgll* expression levels measured by qPCR in the wild-type and mutant MEFs treated with Mock or WNT3A-conditioned media for 24 h. (**e**) Mgll immunohistochemistry in the normal intestinal epithelium (upper panel) and adenoma region (lower panel) in Apc^{Min} mouse small intestine. (**f**) qPCR for *Prdm5* and *Mgll* in mouse jeunum. *P<0.05 according to an unpaired t-test.

Interestingly, *Mgll* is involved in the lipid metabolism and it was identified in our ChIP-seq analysis in Caco-2 cells as a direct PRDM5 target (Figure 3e). Moreover, *Mgll* was recently shown to promote a metabolic program favoring cancer progression.[19] Hence, we focused on this gene as a Prdm5 functional target in colon carcinogenesis. To validate whether *Mgll* is a direct target of Prdm5 also in mouse cells, we performed ChIP-qPCR assays with Prdm5 antibodies in wild-type and *Prdm5*$^{LacZ/LacZ}$ MEFs. Despite failing to identify significant Prdm5 binding around the TSS of *Mgll*, scanning through the gene body of *Mgll* using a number of qPCR primer sets, we identified a Prdm5-binding site inside intron 3 of *Mgll* at 41 kb from the transcription start site (Figure 4c). Interestingly, treatment of wild-type MEFs with media containing WNT3A increased the expression level of *Mgll* and, in *Prdm5*$^{LacZ/LacZ}$ cells, its expression was further upregulated (Figure 4d), suggesting a synergistic effect of Prdm5 loss and WNT signaling activation in *Mgll* regulation and indicating *Mgll* as a novel WNT-responsive gene. Indeed, in *Apc*^{Min} intestine sections, dysplastic regions displayed a higher staining intensity for Mgll compared to areas with normal morphological features (Figure 4e). Importantly, we validated that Prdm5 represses *Mgll* also *in vivo* in the mouse jejunum, as we observed a statistically significant upregulation of *Mgll* transcript upon Prdm5 loss specifically in the small intestine (Figure 4f) and not in the colon (data not shown). Moreover, Mgll protein was upregulated in *Prdm5*$^{LacZ/LacZ}$-*Apc*^{Min} polyps compared to *Apc*^{Min} polyps (Supplementary Figure S1).

Our data demonstrate that Prdm5 targets and regulates *Mgll* in mouse fibroblasts and small intestine. Moreover, *Mgll* is a WNT-responsive gene upregulated synergistically by Prdm5 loss and WNT activation.

Prdm5 protein expression is downregulated in early stages of human colon carcinogenesis

Although a number of studies have demonstrated the frequent promoter methylation of the *PRDM5* gene, no direct observation of PRDM5 protein levels has been estimated in clinical samples. To address this point, we performed immunohistochemical analysis of human colon tissues. We observed an intense PRDM5 expression throughout the colonic epithelium compared with the underlying submucosa (Figure 5a), although PRDM5 was also expressed in endothelial cells, pericytes and smooth muscle (Figure 5b). A closer analysis of the intestinal epithelium reveals a punctate, predominantly nuclear, staining pattern of PRDM5 along the whole epithelial layer in the crypts, with stronger intensity in their apical part (Figure 5c), although we observed defined staining also in cells at the base of the crypts (Figure 5d).

Figure 5.

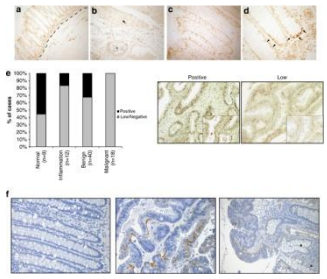

PRDM5 is downregulated in early stages of colon cancer. (**a**–**d**) PRDM5 immunohistochemistry in normal colon tissue samples. (**a**) × 10 magnification. Black dashed line indicates the separation between mucosa and muscularis (**b**–**c**) × 20 magnification displaying muscle tissue in the *tunica muscularis* (area with arrow) and blood vessels (erythrocytes in blood vessels marked with asterisks) and colonic epithelium in the mucosa, respectively. (**d**) × 40 magnification of a colonic crypt. Cells at the base displaying PRDM5 nuclear expression are marked by arrows. (**e**) Left panel: tissue microarray scoring for PRDM5 intensity in epithelial cells. Right panels: representative images of PRDM5 immunohistochemical staining showing a sample of adenoma displaying positive PRDM5 signal (left panel) and low/negative nuclear staining (right panel). (**f**) MGLL immunohistochemistry on normal colon epithelium sample (left panel, × 20) and adenocarcinoma samples (middle panel × 20, right panel × 10). Asterisks indicate region with normal epithelium morphology displaying no MGLL expression.

We next proceeded to perform an immunohistochemical analysis on tissue microarrays containing 80 clinical samples, of which 9 were from normal mucosa, 12 were cases of inflammation (including chronic inflammation and ulcerative colitis), 40 were benign polyps or adenomas and 18 were malignant adenocarcinomas (including grade I (3samples) and grade II (15 samples)). By scoring samples according to the presence of PRDM5 nuclear staining in the epithelium we observed that ~50% of the samples of normal mucosa displayed nuclear staining. Importantly, we found that a significant proportion of the malignant samples had lost PRDM5 expression when compared with the normal mucosal samples (P=0.003, Bonferroni corrected: P=0.009). Furthermore, there was a significant indication of progressive PRDM5 loss during the course of cancer progression, as PRDM5 nuclear expression was more often lost in malignant adenocarcinomas than in benign polyps and adenomas (P=0.012, Bonferroni corrected: P=0.036). We did not detect a significant difference in the number of PRDM5-negative benign samples relative to normal mucosa, probably reflecting the limited size of the data set (Figure 5e). However, when we stained human adenocarcinoma samples with MGLL antibody, we observed the clear expression of MGLL in tumors compared with normal mucosa (Figure 5f) as previously reported,[20] suggesting that *MGLL* could be regulated by PRDM5 in human clinical samples also. Our data demonstrate that PRDM5 is expressed in the human colon epithelium and is downregulated during cancer development.

Discussion

Several studies have implicated PRDM5 as a tumor suppressor based on observed patterns of hypermethylation of the *PRDM5* promoter particularly in colorectal and gastric cancer types[7, 8] and the induction of apoptosis following PRDM5 overexpression in ovarian, breast, liver and gastric cancer cells.[5, 8] Furthermore, PRDM5 was demonstrated to regulate the WNT pathway in zebrafish and human cancer cell lines,[6, 10] and to directly target a series of cancer-relevant loci.[2, 6] In this study, we take a genetic approach and use a *Prdm5* mutant mouse strain to link the loss of Prdm5 expression to the etiology of cancer. Whereas no acceleration of lymphomagenesis was observed in $Trp53^{-/-}$; $Prdm5^{LacZ/LacZ}$ or $Trp53^{+/-}$; $Prdm5^{LacZ/LacZ}$ compound strains, we observed a role for *Prdm5* as a cancer susceptibility gene in the context of intestinal adenomatosis driven by a mutation in the *Apc* tumor-suppressor gene. Apc^{Min} mice hold a mutation that creates an *Apc* truncation at codon 850 and constitutes a functional null allele.[18] The occurrence of intestinal polyps relies on the loss of heterozygosity, in which the wild-type *Apc* allele is

mutated or lost, resulting in hyperactivation of the WNT signaling. By crossing *Prdm5* mutant animals to *Apc*^{Min} mice, we observed an increased number of adenomas in the small intestine, supporting a role for Prdm5 as a negative regulator of the WNT pathway. These results parallel zebrafish studies, in which injection of morpholino oligonucleotides against the *Prdm5* transcript augments the '*masterblind*' phenotype in embryos carrying a heterozygous Axin mutation.[10] Although our cell culture analyses suggest that β-catenin levels are increased in *Prdm5*$^{LacZ/LacZ}$ fibroblasts, substantial differences are seen following *Prdm5* inactivation in zebrafish and mice, such as the absence of obvious developmental defects in *Prdm5* mutant animals.[9]

Towards identifying the mechanistic basis for tumor-suppressive functions of PRDM5, ChIP-sequencing of PRDM5-bound loci in the Caco-2 colon cancer cell line was performed. Caco-2 cells are polarized epithelial cells that grow as normal enterocytes and are often used in drug discovery as models for assaying intestinal epithelial permeability.[21] In line with previous studies, we find PRDM5 to bind a multitude of collagen genes (Supplementary Table S1).[9] In Caco-2 cells, the major collagen targeted is the epithelial *COL4A1*, rather than *COL1A1* as reported in osteoblasts, indicating the cell type-specific target gene recognition of PRDM5. Similarly, we failed to detect the previously published binding to *TWIST1* and *CDK4* promoters.[6] We focus here on PRDM5 target loci involved in metabolic processes, as this gene ontology category was significantly over-represented in the ChIP-seq analysis and is important for cancer development. In the last decade, growing attention has been dedicated to the fact that cancer cells undergo extensive metabolic changes to provide the energy and cell components needed to fuel the increased proliferation and migration.[22, 23, 24] One of the metabolic systems undergoing rapid increase with cellular transformation is the lipogenic pathway.[25] Indeed, fatty acid production is increased in cancer cells due to the upregulation of the fatty acid synthase enzyme.[25] In this study, we show that Prdm5 is a repressor of *Mgll*, and Prdm5 loss acts synergistically with WNT pathway activation in *Mgll* upregulation. Interestingly, *Mgll* is part of the endo-cannabinoid system and it was shown to be a lipolytic enzyme able to free fatty acids, generating pro-oncogenic metabolites such as lipophosphatidic acid and prostaglandins.[19] Indeed, chemical and genetic inhibitions of Mgll impair cancer cell proliferation, migration, invasion and tumor growth in xenograft models,[19, 20, 26] suggesting Mgll as a relevant target for cancer treatment. It is of note that among Prdm5 targets we identified other targets involved in lipid metabolism, such as ATP citrate lyase, which is the enzyme converting citrate to cytosolic acetyl-CoA in the first step of fatty acid synthesis. Importantly, ATP citrate lyase is involved in cellular transformation[27] and its inhibition results in reduced tumor growth.[28] The identification of a metabolic target gene repertoire for PRDM5 points to the relevance of further studies directed towards investigating the metabolic state of Prdm5 mutant tissues particularly following oncogenic stimulation.

In summary, our study provides the first causal link for a tumor-suppressive function of Prdm5. We demonstrate *in vivo* that this function is exerted in the context of *Apc*^{Min}-driven intestinal adenomatosis. By genome-wide analysis of PRDM5-bound loci in human colon cancer cells, we show that PRDM5 targets transcription start sites of metabolic genes and, specifically, that the enzyme *Mgll* is regulated by Prdm5 *in vivo* in the mouse intestine. Moreover, we provide the first analysis of Prdm5 protein downregulation in human colon carcinogenesis.

Materials and methods

Animal experimentation

Prdm5$^{LacZ/LacZ}$ animals were previously described;[9] *Apc*^{Min} mice were obtained from Jackson labs (Bar Harbor, ME, USA) and described elsewhere.[18] For scoring the number of intestinal adenomas, animals were

euthanized at 20 weeks of age, the gastrointestinal tract isolated, flushed with phosphate-buffered saline and immediately fixed in 4% formaldehyde. Intestines were opened longitudinally and adenomas counted macroscopically in a blind manner using a Leica stereoscope (Leica, Heerbrugg, Switzerland). Adenoma diameters were measured using a caliber unit installed in the stereoscope. Histological examination of hematoxylin-and-eosin-stained specimens was performed in a blind manner by an expert pathologist. *p53* mutant animals[17] were euthanized at the occurrence of clinical symptoms and analyzed by gross pathology. All animal experimentations were performed with an approval from the Danish authorities (Dyreforsøgstilsynet, protocol number 2006/562–43).

Cell culture

MEFs were isolated according to standard procedure from E13.5 embryos; all comparisons were performed on clones generated from littermate embryos. L-cells and L-WNT3A cells were purchased from ATCC and maintained in the Dulbecco's modified Eagle medium, 10% fetal bovine serum and 1% penicillin/streptomycin. Conditioned media containing WNT3A and mock media were collected from L-cells and L-WNT3A cells 3 days after reaching confluency, and MEFs were treated with conditioned media for 24 h.

Caco-2 cells (kindly provided by Albin Sandelin, University of Copenhagen, Denmark) were maintained in the Dulbecco's modified Eagle medium, 10% fetal bovine serum and 1% penicillin/streptomycin. Caco-2 cells were transfected with siControl oligo (AllStars Negative Control siRNA, QIAGEN, cat. 1027280, Hilden, Germany) and siPRDM5 (Dharmacon smart pool, cat. M-020332, Hilden, Germany) using DharmaFECT1 (Dharmacon) according to the manufacturer's recommendations and harvested 72 h after treatment.

Gene expression analyses

Cells were lysed in RIPA buffer and immunoblotting performed according to the standard procedures using the antibodies against the following : Prdm5,[9] β-catenin (Cell Signaling, Beverly, MA, USA, 9587), Vinculin (Sigma, St Louis, MO, USA, V9131) and H3 (Cell Signaling, 9715).

Total RNA was extracted from cell pellets using the RNeasy Plus Mini Kit (Qiagen) according to the manufacturer's instructions. Complementary DNA was synthesized using TaqMan Reverse Transcription Reagents (Applied Biosystems, Foster City, CA, USA). qRT–PCR was performed with the One Step plus Sequence Detection System (Applied Biosystems) using the Fast SYBR green master mix reagent (Applied Biosystems). Gene expression levels were normalized to the average of at least two housekeeping genes. Complementary DNA was labeled and hybridized to Affymetrix Mouse Gene 1.0 ST microarrays (Affymetrix, Santa Clara, CA, USA) according to the standard procedure at the Righospitalet microarray facility.

Double-stranded complementary DNA for RNA-sequencing experiments was transcribed using SuperScript Double-Stranded cDNA Synthesis Kit (Invitrogen, Carlsbad, CA, USA) according to the manufacturer's recommendation. Samples were labeled for RNA sequencing and ran on a lane of HiSeq2000 (Illumina, San Diego, CA, USA) at the Danish National High-Throughput DNA Sequencing Centre.

The data have been uploaded to GEO (GSE46821). Real-time PCR primers are provided in Supplementary Table S4.

Chromatin immunoprecipitation and high-throughput sequencing

ChIP assays were performed as previously described.[9] Library generation and sample barcode labeling were obtained using the ChIP-Seq DNA Sample Prep Kit (Illumina) and samples were analyzed on Hi-Seq 2000 (Illumina) at the Danish National High-Throughput DNA Sequencing Centre.

Bioinformatic analyses

The quality of the RNA-seq data was evaluated with fastQC software (www.bioinformatics.babraham.ac.uk/projects/fastqc/). RNA-seq data were analyzed using a pipeline based on the use of TopHat[29] and CuffLinks[30] essentially as previously described.[31] The reference genome used for alignment was hg19 using the UCSC annotation (http://genome.ucsc.edu). Differentially expressed genes were detected using the Bioconductor package Cummerbund[32] and data were represented as FPKM (fragments per kilobase of exon per million fragments mapped). Functional annotation of deregulated genes was performed using DAVID (http://david.abcc.ncifcrf.gov/).

For ChIP-seq, reads were mapped over the hg19 assembly of the human reference genome using Bowtie2 software[33] set for a local alignment, keeping only the best alignment available for each read. The numbers of aligned reads were: 38.2×10^6 (87.78%) for Prdm5-Ab1, 28.3×10^6 (86.80%) for Prdm5-Ab2 and 31.5×10^6 reads (51.85%) for immunoglobulin G control. Peak calling and filtering were run on the mapping data using MACS software and ChIPpeakAnno package from Bioconductor as previously described.[9] A total of 2970 peaks were found for Prdm5-Ab1 and 2594 for Prdm5-Ab2, with a total of 1413 overlapping peaks between the two sets. Annotation leads to a categorization of peaks on the basis of the relative position in respect to the gene (upstream, intragenic, downstream and TSS, the latter defined as a range from −1 kb to +1 kb from the annotated transcription start site). Functional annotation and gene ontology enrichment of annotated genes were performed using GREAT (http://bejerano.stanford.edu/great/public/html/).

For microarray analysis, two conditions were investigated: wild-type MEFs and *Prdm5*$^{LacZ/LacZ}$ MEFs, and for experimental condition biological triplicates were analyzed. Microarray quality control and statistical validation were performed using Bioconductor.[32] Probe set intensities were obtained by means of RMA[34] and normalization was carried out according to the quantiles method. The number of genes evaluated was reduced by applying an interquartile filter (out of 35 556 probe sets, 7562 probe sets, with interquartile >0.25, were retained) to remove the nonsignificant probe sets (that is, those not expressed and those not changing). Differential gene expression was detected using an empirical Bayes method.[35] OneChannelGUI graphical interface package was used to run any of the described analysis.[36]

Tissue immunostaining

Two anti-Prdm5 affinity-purified antibodies previously described[9] were tested for immunohistochemistry on normal human colon tissues (kindly provided by Francesca Molinari and Milo Frattini, IOSI, Bellinzona, Switzerland) and specificity was assessed by common staining pattern and pre-adsorption with recombinant antigen.

Tissue microarrays were obtained from Biomax (Rockville, MD, USA) (cat. CO809) and stained with PRDM5 antibodies according to the standard procedure. The TMAs were blinded and scored for the detection of epithelial cells showing nuclear PRDM5 signal (positive samples are considered when >20% of the epithelium display nuclear PRDM5 signal).

Mouse intestines were embedded and Mgll immunostaining was performed according to the standard procedure using Mgll antibody (Abcam, Cambridge, MA, USA, ab24701).

References

1. Fog CK, Galli GG, Lund AH. PRDM proteins: important players in differentiation and disease. Bioessays 2012; 34: 50–60.

2. Duan Z, Person RE, Lee HH, Huang S, Donadieu J, Badolato R *et al*. Epigenetic regulation of protein-coding and microRNA genes by the Gfi1-interacting tumor suppressor PRDM5. Mol Cell Biol 2007; 27: 6889–6902.

3. Burkitt Wright EM, Spencer HL, Daly SB, Manson FD, Zeef LA, Urquhart J *et al*. Mutations in PRDM5 in brittle cornea syndrome identify a pathway regulating extracellular matrix development and maintenance. Am J Hum Genet 2011; 88: 767–777.

4. Cheng HY, Chen XW, Cheng L, Liu YD, Lou G. DNA methylation and carcinogenesis of PRDM5 in cervical cancer. J Cancer Res Clin Oncol 2010; 136: 1821–1825.

5. Deng Q, Huang S. PRDM5 is silenced in human cancers and has growth suppressive activities. Oncogene 2004; 23: 4903–4910.

6. Shu XS, Geng H, Li L, Ying J, Ma C, Wang Y *et al*. The epigenetic modifier PRDM5 functions as a tumor suppressor through modulating WNT/beta-catenin signaling and is frequently silenced in multiple tumors. PLoS One 2011; 6: e27346.

7. Watanabe Y, Kim HS, Castoro RJ, Chung W, Estecio MR, Kondo K *et al*. Sensitive and specific detection of early gastric cancer with DNA methylation analysis of gastric washes. Gastroenterology 2009; 136: 2149–2158.

8. Watanabe Y, Toyota M, Kondo Y, Suzuki H, Imai T, Ohe-Toyota M *et al*. PRDM5 identified as a target of epigenetic silencing in colorectal and gastric cancer. Clin Cancer Res 2007; 13: 4786–4794.

9. Galli GG, Honnens de Lichtenberg K, Carrara M, Hans W, Wuelling M, Mentz B *et al*. Prdm5 regulates collagen gene transcription by association with RNA polymerase II in developing bone. PLoS Genet 2012; 8: e1002711.

10. Meani N, Pezzimenti F, Deflorian G, Mione M, Alcalay M. The tumor suppressor PRDM5 regulates Wnt signaling at early stages of zebrafish development. PLoS One 2009; 4: e4273.

11. Reya T, Clevers H. Wnt signalling in stem cells and cancer. Nature 2005; 434: 843–850.

12. Groden J, Thliveris A, Samowitz W, Carlson M, Gelbert L, Albertsen H *et al*. Identification and characterization of the familial adenomatous polyposis coli gene. Cell 1991; 66: 589–600.

13. Kinzler KW, Vogelstein B. Lessons from hereditary colorectal cancer. Cell 1996; 87: 159–170.

14. Clevers H. Wnt/beta-catenin signaling in development and disease. Cell 2006; 127: 469–480.

15. Sansom OJ, Reed KR, Hayes AJ, Ireland H, Brinkmann H, Newton IP *et al*. Loss of Apc *in vivo* immediately perturbs Wnt signaling, differentiation, and migration. Genes Dev 2004; 18: 1385–1390.

16. Nathke IS. The adenomatous polyposis coli protein: the Achilles heel of the gut epithelium. Annu Rev Cell Dev Biol 2004; 20: 337–366.

17. Purdie CA, Harrison DJ, Peter A, Dobbie L, White S, Howie SE *et al*. Tumour incidence, spectrum and ploidy in mice with a large deletion in the p53 gene. Oncogene 1994; 9: 603–609.

18. Moser AR, Pitot HC, Dove WF. A dominant mutation that predisposes to multiple intestinal neoplasia in the mouse. Science 1990; 247: 322–324.

19. Nomura DK, Long JZ, Niessen S, Hoover HS, Ng SW, Cravatt BF. Monoacylglycerol lipase regulates a fatty acid network that promotes cancer pathogenesis. Cell 2010; 140: 49–61.

20. Ye L, Zhang B, Seviour EG, Tao KX, Liu XH, Ling Y *et al*. Monoacylglycerol lipase (MAGL) knockdown inhibits tumor cells growth in colorectal cancer. Cancer Lett 2011; 307: 6–17.

21. Hidalgo IJ, Raub TJ, Borchardt RT. Characterization of the human colon carcinoma cell line (Caco-2) as a model system for intestinal epithelial permeability. Gastroenterology 1989; 96: 736–749.

22. DeBerardinis RJ, Lum JJ, Hatzivassiliou G, Thompson CB. The biology of cancer: metabolic reprogramming fuels cell growth and proliferation. Cell Metab 2008; 7: 11–20.

23. Deberardinis RJ, Sayed N, Ditsworth D, Thompson CB. Brick by brick: metabolism and tumor cell growth. Curr Opin Genet Dev 2008; 18: 54–61.

24. Hanahan D, Weinberg RA. Hallmarks of cancer: the next generation. Cell 2011; 144: 646–674.

25. Menendez JA, Lupu R. Fatty acid synthase and the lipogenic phenotype in cancer pathogenesis. Nat Rev Cancer 2007; 7: 763–777.

26. Nomura DK, Lombardi DP, Chang JW, Niessen S, Ward AM, Long JZ *et al*. Monoacylglycerol lipase exerts dual control over endocannabinoid and fatty acid pathways to support prostate cancer. Chem Biol 2011; 18: 846–856.

27. Bauer DE, Hatzivassiliou G, Zhao F, Andreadis C, Thompson CB. ATP citrate lyase is an important component of cell growth and transformation. Oncogene 2005; 24: 6314–6322.

28. Hatzivassiliou G, Zhao F, Bauer DE, Andreadis C, Shaw AN, Dhanak D *et al*. ATP citrate lyase inhibition can suppress tumor cell growth. Cancer Cell 2005; 8: 311–321.

29. Kim D, Salzberg SL. TopHat-Fusion: an algorithm for discovery of novel fusion transcripts. Genome Biol 2011; 12: R72.

30. Roberts A, Pimentel H, Trapnell C, Pachter L. Identification of novel transcripts in annotated genomes using RNA-Seq. Bioinformatics 2011; 27: 2325–2329.

31. Trapnell C, Roberts A, Goff L, Pertea G, Kim D, Kelley DR *et al*. Differential gene and transcript expression analysis of RNA-seq experiments with TopHat and Cufflinks. Nat Protoc 2012; 7: 562–578.

32. Gentleman RC, Carey VJ, Bates DM, Bolstad B, Dettling M, Dudoit S *et al*. Bioconductor: open software development for computational biology and bioinformatics. Genome Biol 2004; 5: R80.

33. Langmead B, Salzberg SL. Fast gapped-read alignment with Bowtie 2. Nat Methods 2012; 9: 357–359.

34. Irizarry RA, Hobbs B, Collin F, Beazer-Barclay YD, Antonellis KJ, Scherf U *et al*. Exploration, normalization, and summaries of high density oligonucleotide array probe level data. Biostatistics 2003; 4: 249–264.

35. Smyth GK. Linear models and empirical bayes methods for assessing differential expression in microarray experiments. Stat Appl Genet Mol Biol 2004; 3: Article3.

36. Sanges R, Cordero F, Calogero RA. oneChannelGUI: a graphical interface to Bioconductor tools, designed for life scientists who are not familiar with R language. Bioinformatics 2007; 23: 3406–3408.

Acknowledgements

We would like to acknowledge Julia Sidenius Johansen for her advice on TMA stainings, Bettina Mentz for excellent technical assistance and Fengqin Jia for mouse genotyping. This work was supported by the Danish National Research Foundation, the Danish National Advanced Technology Foundation, the Novo Nordisk Foundation, the EC FP7 programs (ONCOMIRS, grant agreement number 201102), the Lundbeck Foundation and the Danish Cancer Society.